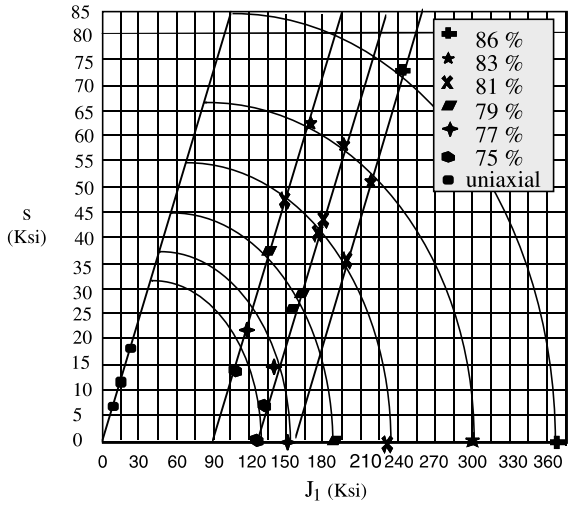

Fig. 9. Fitting of the cap surfaces and the shear failure surface.

those related to the material hardening law. The range of variation for all the parameters was taken as ±5% around the set value except for parameter K_0 and for the shear failure parameters which had null set values. For these last parameters, larger variation ranges were required in order to obtain a significant perturbation of the model results (Ross, 1988). All these simulations were concerned with a simple cylindrical slug subjected to rigid die compaction with ideal frictionless die contact.

Table 1 summarizes the preliminary model parameter values obtained for the 316L stainless steel powder, as well as their respective relative influence on the final density distribution in a compact, as determined by the sensitivity analysis. It should be noted that the cap initial position was not determined experimentally but was simply taken as a very small value, implying that the powder had no elastic behavior when in the loose state.

3.6. Validation of the material parameter set

A series of FE simulations were carried out in order to validate the material parameters. These simulations are aimed at reproducing the experimental tests, namely the isostatic and the triaxial compaction tests, used to calibrate the model. The simulations were based on a single axisymmetric element mesh,

Table 1
Values and relative influence of the 316L parameters

Parameters	Units	Values	Relative influence (%)
E	ksi	Function (Fig. 4)	19.32
G	ksi	Function (Fig. 4)	11.29
α	ksi	0	0.83
β	ksi^{-1}	0	0.06
γ	ksi	0	0.68
θ	–	0.617	0.32
W	–	0.916	54.47
D	ksi^{-1}	0.00197	12.21
R	–	Function (Eq. (18))	0.64
K_0	ksi	0.001	0.01

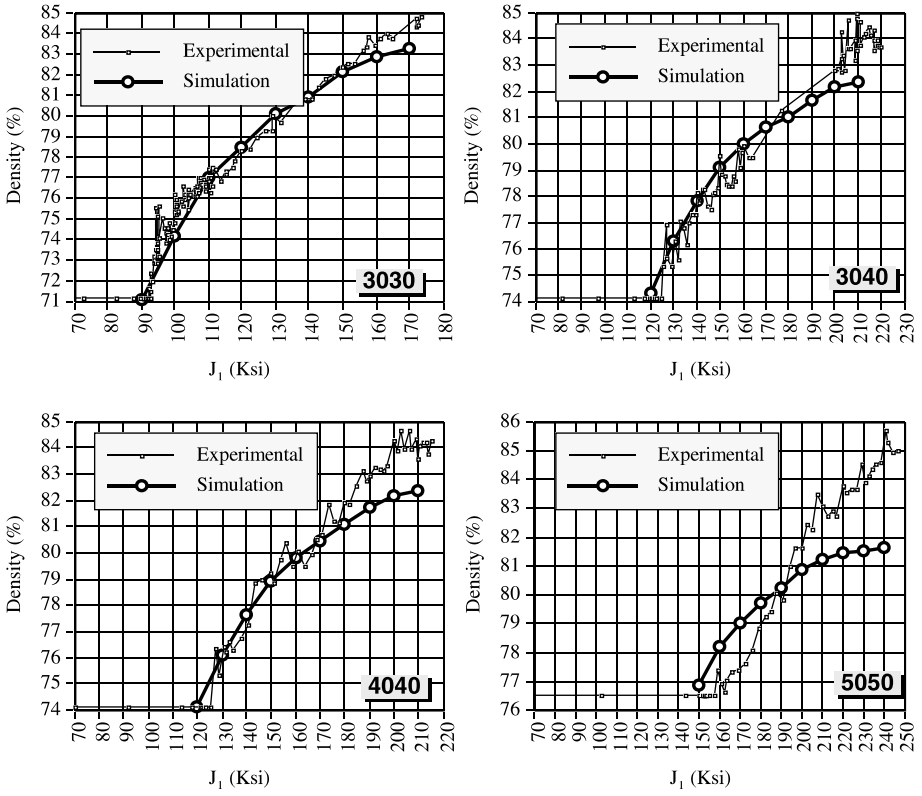

Fig. 10. Simulation results of the triaxial compression tests.

subjected to imposed pressures corresponding to experimental conditions. The results of the two series of simulation are graphically shown, in terms of achieved relative density, in Figs. 10 and 11.

As shown in these figures, a good agreement between experimental and simulated results was achieved for most cases. In fact, except for the 5050 triaxial compaction test, discrepancy never exceeded 1.5% (in

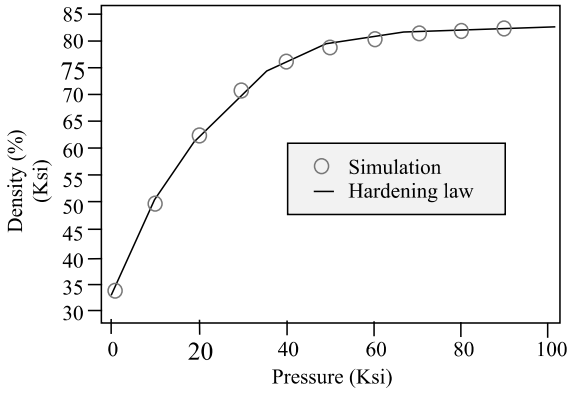

Fig. 11. Simulation results of the isostatic compression tests.

terms of relative density). The higher discrepancy that appears only at the late stages of compression is due to an approximation used in processing the triaxial tests data and hence does not result from an eventual inaccuracy of the model. In fact, as mentioned earlier, it was assumed, for a preliminary data analysis, that once the pre-compaction pressure is reached, all subsequent deformation is totally plastic. However, it appears that accumulated elastic strain, which should not be accounted for in density calculation, is not as small as we assumed, but can reach as much as 3%. This explains why the experimental density is as much as higher than the predicted one.

Globally, the results obtained from the model are largely acceptable, knowing that the experimental tests involved considerable noise (Ross, 1988). Accordingly, the obtained values for the material parameters are considered to be valid and are retained for the rest of simulations.

4. Experimental validation technique

4.1. Overview

Different techniques for local density evaluation have been developed and proposed for the last twenty years. Generally, these techniques were compared to bulk density measurements (e.g. wet/dry technique) taken on part samples of supposedly constant density. Unfortunately, most if not all of these local density evaluation techniques are still under development for reason of considerable measurement variability that is caused in turn by inadequate control of sample preparation and testing.

Because local density can be correlated to part conductivity, hardness and several other more easily measured properties, indirect techniques have grown in popularity. In a previous research (Guillot et al., 1995), we reviewed the most commonly used methods. We also established the sensitivity of factors involved during sample preparation and testing, attempted to improve the technique and assessed the accuracy, for two promising local density evaluation techniques: (1) Vickers hardness and (2) analysis of images obtained using an optical microscope. Even though excellent results were obtained with both techniques, the first is chosen in practical applications due to its less demanding experimental protocol. The basic elements of this protocol are presented in the remaining part of this section.

4.2. Sample preparation

Samples of 2 cm diameter by 0.7 cm height were compacted into a billet shape. Pressing ranging between 20 and 60 tsi (tons per square inch) provided billets of different density levels. The green compacts were lightly sintered to remove the lubricant and to improve strength for sectioning and metallographic sample preparation. However, it was important to avoid the alteration of their densities. Consequently, each billet was sintered in 100% H_2 atmosphere for 30 min at 450 °C temperature. Then, density was determined as the weight divided by the volume as measured with a micrometer.

In addition, the billets were cut using a diamond wheel and both cut sections were mounted in a Lucite mounting cup. Afterwards, samples were ground and polished on a versatile grinder-polisher with room for six samples and rotating at 30 rpm, following the conditions of Table 2.

4.3. Vickers hardness measurements and correlation with density

This Vickers hardness measurement technique was used to obtain apparent hardness also called macrohardness, i.e. the average hardness of a porous material. Its procedure is well documented in ASTM E92-82 standard (ASTM, 1987). This standard offers various loading from 1–120 kgf applied to an indenter of pyramidal geometry with face angle of 136°. In this work, a 5 kgf load (HV 5) was used as recommended in

Table 2
Polishing conditions

	Grinding	Polishing		
		Rough	Medium	Fine
Material	180 grit	320 grit	600 grit	5 μ alumine
Passing weight	1 lb	1 lb	1 lb	1 lb
Time	Until surface flat and without defect	1.5 min	1.5 min	2.0 min

Table 3
Correlation between density and Vickers hardness

Experiment	Billet green density (%)	Vickers hardness HV (kg/mm^2)			
		Average		Standard deviation	
		Face A	Face B	Face A	Face B
1	77.9	44.3	46.2	2.58	2.22
2	80.3	54.6	54.3	4.38	2.26
3	82.0	61.8	62.6	2.69	2.18
4	84.2	71.1	71.7	4.23	1.92
5	86.3	81.5	81.5	2.64	2.64

MPIF standard 43 (MPIF, 1991). Measurements were performed on five billets of different densities. Each billet had two faces on which $n = 15$ hardness measurements were realized in a 3×5 pattern. The results are reported in Table 3.

As shown in Fig. 12, the relationship between the green density and the logarithm of Vickers hardness can be correlated with a linear model. Using a linear regression technique, the density of green compacts (GC) becomes:

$$\text{Density } (\%) = \rho_{\text{HV,GC}} = 32.72 \ \log(\text{HV}) + 23.56 \tag{18}$$

Error limits introduced by this model, by sample preparation factors and by the hardness measurements can be established to $\pm(0.05 + 7.8/n)^{1/2}$ with a confidence level of 68%. Curiously, most of the error is caused by the Vickers measurement, and thus, can significantly be reduced by taking and averaging "n" measurements in a small area.

Thus, to obtain the local density distribution in any compact made of the studied powder, this part should first be prepared following the presented experimental protocol. Then, Vickers hardness measure-

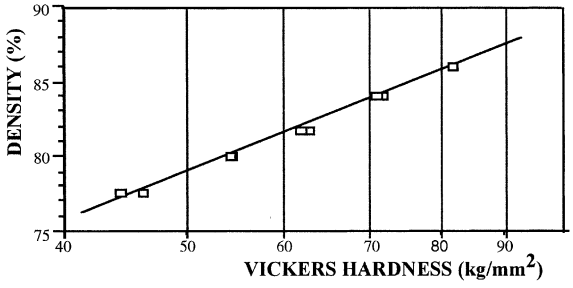

Fig. 12. Linear relationship between density and Vickers hardness.

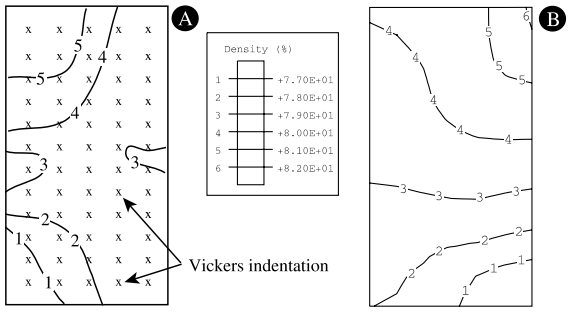

Fig. 13. (A) Experimental vs (B) simulation results.

ment could be taken and translated into density measurements using the established calibration curve. Finally, it was proved that this technique could be applied with a similar accuracy to other powder materials (Guillot and Chtourou, 1996).

5. Application

A simple cylindrical part made of 316L stainless steel powder was pressed on an a 50 ton mechanical press. The tooling needed to press this part consisted of a die, a lower punch and an upper punch. An axisymmetric model of this application was used to determine the final density distribution in the compact.

Besides, an integrated simulation module, designed so as to render the modeling approach practical and industrially usable, was developed. This module permits an easy definition of the tooling and the powder geometry, as well as the compaction sequence and all other boundary conditions. It also handles FE solution and results post processing. [3] The density distribution obtained after the three step compaction sequence compares well to the experimental density map (Fig. 13). This map was obtained by the way of a specially developed method based on the correlation of local density and Vickers macro-hardness.

6. Conclusion

This paper addressed the material characterization and validation of a particular cap model originally developed to deal with geological materials and properly adapted so as to handle ductile metal powders. An experimental characterization procedure has been developed and applied for the case of 316L stainless steel powder. The obtained material parameter set was validated by way of the simulation of the characterization tests and served as a basis for the model parameters sensitivity analysis. This study proved that the imperfections of the procedure do not affect the most influent parameters.

In addition, an experimental technique for the evaluation of the local density distribution was developed in order to validate the simulation results. This technique, based on a correlation with Vickers macrohardness measurements, permits an accuracy of 1% in terms of relative density. An integrated simulation module, developed in a related research was also used to run a simulation of the compaction of an industrial PM part. The comparison of the obtained density distribution with an experimentally measured map served as a validation for the modeling approach.

[3] Through the software Abaqus and Abaqus-Post respectively.

Presently, our main research orientations are the improvement of the model characterization procedure to include a better description of the powder elastic behavior. Furthermore, 3D simulation module, capable of modeling general non-axisymmetric applications, is under development.

Acknowledgements

The authors would like to thank Mr. Sébastien Parent and Ms. Isabelle Jacob from Précitech Inc. for the experimental assistance as well as M. Christian Michaud, Mrs. Cathryn Macrander and M. André Hengartner for their help in software development. The authors would also like to acknowledge the support of the National Sciences and Engineering Research council of Canada (strategic grant nos. 0167091 and CRD-186296).

References

Alm, O., 1983. Mechanical testing of powders and powder compacts. Scandinavian Journal of Metallurgy 12, 302–311.

ASTM, 1987. Standard E92-82, Standard Test Method for Vickers Hardness of Metallic Materials.

Biba, N.V., Keife, H., Sthalberg, U., 1993. A finite element simulation of powder compaction confirmed by model-material experiment. Journal of Materials Processing Technology 36, 141–155.

Brown, S., Abou-Chedid, G., 1993. Evaluation of yield functions due to powder characteristics. Advances in Powder Metallurgy and Particulate Materials 3, 245–255.

Chtourou, H., 1996. Modélisation par Éléments Finis du Procédé de Compression des Poudres Métalliques de l'Acier Inoxydable 316-L. Ph.D. Thesis, Laval University, Quebec.

Chtourou, H., Guillot, M., Gakwaya, A., 1995. Modeling the rigid die compaction of 316L stainless steel powder. Advances in Powder Metallurgy and Particular Materials 1 (2), 169–183.

Crawford, J., Lindskog, P., 1983. Constitutive equations and their role in the modeling of the cold pressing process. Scandinavian Journal of Metallurgy 12, 271–281.

Dimaggio, F., Sandler, I., 1971. Material model for granular soils. Journal of the Engineering Mechanics Division, 935–950.

Doraivelu, S.M., Gegel, H.L, Gunasekera, J.S, Malas, J.C., Morgan, J.T., Thomas, J.F., 1984. A new yield function for compressible P/M materials. International Journal of Mechanical Sciences 26, 527–535.

German, R.M., 1984. Powder Metallurgy Science. MPIF, Princeton, NJ.

Guillot, M., Chtourou, H., 1996. Generalization of the Vickers hardness local density measurement technique to different powder materials, Proceedings of the World Congress on Powder Metallurgy and Particulate Materials, vol. 1, part 4, Washington DC, pp. 31–40.

Guillot, M., Chtourou, H., Parent, S., 1995. Modeling the rigid die compaction of 316L stainless steel powder. Advances in Powder Metallurgy and Particular Materials 3 (9), 31–49.

Gurson, A.L., Posteraro, R.A., 1992. Yield functions for metal powders for use in the numerical simulation of powder compaction, TMS Conference, San Diego CA.

Hofstetter, G., Simo, J.C., Taylor, R.L., 1993. A modified Cap model: closest point solution algorithms. Computers and Structures 46 (2), 203–214.

Innovare Inc. 1993. Advanced Metalworking System, Bath, PA, vol. 114, no. 2.

Jagota, J., Dawson, P.R., 1988a. Micromechanical modeling of powder compacts-I. Unit problems for sintering and traction induced deformation. Acta Metallurgica 36 (9), 2551–2561.

Jagota, J., Dawson, P.R., 1988b. Micromechanical modeling of powder compacts-II. Truss formulation of discrete packing. Acta Metallurgica 36 (9), 2563–2573.

Koopman, M.G., Rachakonda, V.B.S., Gurson, A.L., McCabe, T., 1992. Material models for the finite element simulation of compaction of metal powder, TMS Fall Meeting, Chicago.

Kuhn, A.H., Downey, C.L., 1971. Deformation characteristics and plasticity theory for sintered powder materials. International Journal of Powder Metallurgy 7 (1), 15–25.

Lenel, F.V., 1980. Powder Metallurgy, Principles and Applications. MPIF, Princeton, NJ.

MPIF, Standard 04, 1992. Using the Hall Apparatus, Determination of Apparent Density of free Flowing Metal Powders, Princeton, NJ.

MPIF, Standard 42, 1986. Determination of Density of Compacted and Sintered Metal Powder Products, Princeton, NJ.

MPIF, Standard 43, 1991. Method for Determination of Hardness of Powder Metallurgy Products.
Ross, P.J., 1988. Taguchi Techniques for Quality Engineering. McGraw-Hill, New York.
Sandler, I.S., Rubin, D., 1979. An algorithm and a modular subroutine for the Cap model. International Journal for Numerical and Analytical Methods in Geomechanics 3, 173–186.
Shima, S., Oyane, M., 1976. Plasticity theory for porous material. International Journal of Mechanical Science 18, 285–291.
Shima, S., Saleh, M.A.E., 1993. Variation of density distribution in compacts in closed die compaction with powder characteristics. Advances in Powder Metallurgy and Particulate Materials 3, 175–189.
Simo, J.C., Ju, J.W., Pister, K.S., Taylor, R.L., 1988. Assessment of Cap model: consistent return algorithms and rate dependent extension. ASCE Journal of Engineering Materials 114 (2), 191–218.
Spinner, S., Tefft, W.E., 1961. ASTM proceedings, Engineering, p. 1221.
Trasorras, J., Krauss, T.M., Fergusson, B.L., 1989. Modeling the powder compaction using the finite element method, Proceedings of the 1989 International Conference on Powder Metallurgy, San Diego, CA, pp. 85–104.
Weber, G.G., Brown, S.B., 1989. Simulation of the compaction of powder components. Advances in Powder Metallurgy and Particulate Materials 1, 105–118.
Yu, C.J., Henry, R.J., Prucher, T., Parthasarathi, S., Jo J., 1992. Reasonant frequency measurements for the determination of elastic properties of P/M components, Proceedings of the P/M'92 World Congress, vol. 6, pp. 319–332.